

High-Contrast 3.8 Micron Imaging Of The Brown Dwarf/Planet-Mass Companion to GJ 758

Thayne Currie¹, Vanessa Bailey², Daniel Fabrycky³, Ruth Murray-Clay³, Timothy Rodigas², Phil Hinz²

ABSTRACT

We present L' band ($3.8\ \mu m$) MMT/Clio high-contrast imaging data for the nearby star GJ 758, which was recently reported by Thalmann et al. (2009) to have one – possibly two– faint comoving companions (GJ 758B and “C”, respectively). GJ 758B is detected in two distinct datasets. Additionally, we report a *possible* detection of the object identified by Thalmann et al as “GJ 758C” in our more sensitive dataset, though it is likely a residual speckle. However, if it is the same object as that reported by Thalmann et al. it cannot be a companion in a bound orbit. GJ 758B has a H-L' color redder than nearly all known L–T8 dwarfs. Based on comparisons with the COND evolutionary models, GJ 758B has $T_e \sim 560\ K^{+150K}_{-90K}$ and a mass ranging from $\sim 10\text{--}20\ M_J$ if it is ~ 1 Gyr old to $\sim 25\text{--}40\ M_J$ if it is 8.7 Gyr old. GJ 758B is likely in a highly eccentric orbit, $e \sim 0.73^{+0.12}_{-0.21}$, with a semimajor axis of $\sim 44\ AU^{+32AU}_{-14AU}$. Though GJ 758B is sometimes discussed within the context of exoplanet direct imaging, its mass is likely greater than the deuterium-burning limit and its formation may resemble that of binary stars rather than that of jovian-mass planets.

Subject headings: planetary systems, stars: brown dwarfs, techniques: high angular resolution

1. Introduction

High-contrast imaging surveys have recently identified many faint, cool companions to nearby stars whose inferred masses are between that of Jupiter and the deuterium burning limit ($\sim 13\ M_J$). The companions to nearby A stars – HR 8799, Fomalhaut, and β Pic

¹NASA-Goddard Space Flight Center

²Steward Observatory, University of Arizona

³Harvard-Smithsonian Center for Astrophysics

– orbit at separations less than ~ 100 AU, have small mass ratios, and generally resemble scaled-up versions of gas giant planets in our solar system (Marois et al. 2008a; Kalas et al. 2008; Lagrange et al. 2010), with temperatures that are (likely) $\lesssim 1500$ K (Marois et al. 2008a; Hinz et al. 2010; Currie et al. 2010a), comparable to that for many L and T dwarfs (e.g. Metchev et al. 2006; Leggett et al. 2010).¹ Other directly imaged companions have similar temperatures but orbit low-mass stars and brown dwarfs, typically at wider separations and/or with much larger mass ratios (e.g. Chauvin et al. 2004; Itoh et al. 2005; Luhman et al. 2006; Lafreniere et al. 2010; Todorov et al. 2010), indicating that they plausibly represent the low-mass tail of objects formed by molecular cloud core or protostellar disk fragmentation (e.g. Lodato et al. 2005). The planetary companions to A stars pose strong challenges for even the most efficient core accretion models of gas giant planet formation, given the difficulty of forming massive cores at 10–100 AU (e.g. Rafikov 2010) prior to the dispersal of the protoplanetary disk. The configuration of at least one system with a low-mass primary and planet-mass companion, 2MASS J04414489+2301513, implies that the fragmentation of molecular cloud cores can produce objects $\lesssim 5\text{--}10 M_J$, below the classical “opacity-limited” minimum fragmentation mass (Todorov et al. 2010).

The faint companion and candidate companion to the nearby star GJ 758 reported by Thalmann et al. (2009; hereafter T09), GJ 758B and “GJ 758C”, present an intriguing contrast to planets orbiting A stars and to other substellar-mass L/T dwarfs. GJ 758 is much later in spectral type (G8V) and lower in mass ($M_\star = 0.97 \pm 0.03 M_\odot$, Takeda et al. 2007) than HR 8799, Fomalhaut, and β Pic ($1.5\text{--}2.1 M_\odot$). On the other hand, the projected separation for GJ 758B ($1.858''$, PA = 198.18° on 2009 Aug. 6, or ~ 29 AU) and “GJ 758C” ($1.118''$, PA = 219.16° , or ~ 18 AU) are comparable to the separations for planets orbiting HR 8799 and β Pic (Marois et al. 2008a; Lagrange et al. 2010) and within the brown dwarf desert (e.g. Kraus et al. 2008). Based on GJ 758B’s H band magnitude and age (0.7–8.7 Gyr), T09 argue that the companion likely has a temperature of 549–637 K ($M = 11.7\text{--}48.5 M_J$), making it the coldest known companion to a Sun-like star. Since T09 image the system only in H band, the companion’s temperature –and thus luminosity – remain observationally unconstrained. Inferred masses critically depend on these properties, so new longer wavelength data help constrain whether GJ 758B better resembles the low mass-ratio planetary companions to A stars or high mass-ratio binary star companions to lower-mass stars.

Here we report the L’ band detection of GJ 758B and candidate detection of “GJ 758C” with the Clio camera at the 6.5m MMT telescope. Combined with the H band photometry

¹Dynamical constraints for the masses of some of these companions – e.g. those orbiting HR 8799 – are consistent with luminosity-derived estimates (Chiang et al. 2009; Fabrycky and Murray-Clay 2010)

from T09, we estimate the temperature, luminosity, and mass of GJ 758B. Combining all astrometric datapoints for GJ 758B, we determine its range of allowed orbits.

2. Observations and Data Reduction

GJ 758 was imaged under photometric conditions on May 27, 2010 and June 2, 2010 at the 6.5m MMT telescope with the upgraded Clio mid-IR camera (Hinz et al. 2006; Sivanandam et al. 2006). As described in online documentation², the new Clio detector (Clio-2) operates from $1.65\ \mu\text{m}$ to $4.8\ \mu\text{m}$, covering standard Mauna Kea filters and narrow-band filters centered on wavelengths between 3 and $4\ \mu\text{m}$. Both sets of data reported here were obtained in the L' filter ($3.8\ \mu\text{m}$). All data was taken in *angular differential imaging* mode (Marois et al. 2006), which keeps the instrument rotator fixed, allowing the field of view to rotate with time. The May data consist of coadded frames of 9s each for a total integration time of 2520s. The data were taken through transit, yielding a total field rotation of 192 degrees. The June data consist of coadded frames of 9.6s each for a total integration time of 1536s but were obtained well after transit for a total field rotation of 16.7 degrees. In both datasets, the star was dithered along the detector by 5–10" every 48–90s for sky subtraction. For precise astrometric calibration during our run, we observed the double stars HIP 88817/88818 and HD 223718. The detector orientation is offset by $2.53^\circ \pm 0.15^\circ$ counterclockwise from true north along the y axis; the pixel scale is $0.029915 \pm 8 \times 10^{-5}$ "/pixel. Independent astrometry performed by multiple coauthors confirm these values. Based on this pixel scale, our image FWHM is $\sim 0.15''$ for both datasets.

Our image processing method closely followed the ADI/LOCI (Angular Differential Imaging/Locally-Optimized Combination of Images) reduction procedure described by Marois et al. (2006, 2008a) and Lafreniere et al. (2007) used to maximize the companion signal relative to speckle-dominated noise. The subtracted residual images produced by our ADI/LOCI pipeline were then derotated, median combined, and convolved with a gaussian kernel equal to the image FWHM to produce final science images. Separately from our LOCI reduction, we performed a simple ADI reduction by derotating, high-pass filtering, and median combining the PSF subtracted images (e.g. Hinz et al. 2010).

Figure 1 shows the final reduced images for the May dataset (left) and June dataset (right) produced with the LOCI pipeline. The May dataset clearly reveals a point source at a separation of $1.823'' \pm 0.015''$ ($a_{\text{proj}} \sim 28.4\ \text{AU}$) and position angle of 199.76 ± 0.15 degrees. Within astrometric errors, we identify a point source at the same position in the

²<http://zero.as.arizona.edu/wiki/doku.php>

lower-quality June data ($1.827'' \pm 0.043''^3$), indicating that its detection is secure. We recover the point source in our more simple ADI reductions as well. This separation is comparable to that for GJ 758B as reported by T09 ($1.858'' \pm 0.005''$); the difference in position angle ($\delta(\text{PA}) = 1.58^\circ$) is consistent with an object undergoing counterclockwise motion with respect to the primary. The velocity in the plane of the sky of GJ 758B, derived by comparing our May 2010 position with previously reported positions (T09), is 1.3 ± 0.2 AU/yr. This is less than the minimum escape velocity at this projected separation ($1.64 \pm 0.03 \text{ AU/yr} \times (M_\star/0.97M_\odot)^{1/2} \times (a_p/28.50 \text{ AU})^{-1/2}$), suggesting a bound orbit. Thus, we conclude that we have detected GJ 758B.

The LOCI reduction of the May data also reveals a second, candidate point source at $1.101'' \pm 0.015''$, comparable to that reported for the candidate companion, “GJ 758C”, in T09. However, the large difference in position angle ($\sim 20^\circ$) would imply a space velocity of 7.9 ± 0.3 AU/yr, nearly four times greater than the escape velocity of 2.08 AU/yr. Thus, if our candidate point source is “GJ 758C”, it cannot be in a bound orbit around the primary.

To assess the significance of the GJ 758B detection and candidate “GJ 758C” detection, we compute the standard deviation and signal-to-noise of pixel values in concentric annuli (e.g. T09). The signal-to-noise is ~ 6.4 at GJ 758B’s position and ~ 3 at the candidate “GJ 758C” position. Thus, the signal-to-noise of our possible “GJ 758C” detection is only marginally significant ($\sim 3\sigma$), even though it is locally well separated from large background fluctuations. Bona-fide detections in speckle-noise limited regions typically need to be greater than 5σ in order to rule out false “detections” from residual speckles (Marois et al. 2008b). Because of the chance that “GJ 758C” could be a residual speckle and the lack of a detection in our June data, we consider the second point source in our May data to only be a *candidate* detection of the point source identified by T09 as “GJ 758C”⁴ Since only the detection of GJ 758B is secure, we focus on it in our analysis.

³The much larger error bars result because the companion is contaminated by some residual speckle noise

⁴Chance superpositions of substellar objects close to stars like GJ 758 with L’ band brightnesses similar to our candidate detection are unlikely to be frequent. Assuming a flat substellar mass function ($\alpha = 0$) with a space density described in Table 4 of Burgasser et al. (2004) using the absolute magnitude vs. spectral type of L/T dwarfs at the Spitzer/IRAC [3.6] band from Leggett et al. (2010) as a proxy for L’ brightness, the probability of contamination by a background brown dwarf with $T_e = 500\text{--}1500$ K is $< 10^{-3} \%$.

3. Photometric and Astrometric Analysis

Photometry for GJ 758B from the May data was performed with IDLPHOT, using a 2.5 pixel aperture radius and a background annulus between 2.5 and 5 pixels. In all exposures, the stellar PSF core is saturated. For photometric calibration, we compare the GJ 758B flux to that for HD 223718A, which was observed immediately after GJ 758. HD 223718A is an F5V star ($T_e \sim 6440$ K, Currie et al. 2010b) and should have $K-L' = 0.04$ (Tokunaga 2000). Based on its 2MASS photometry ($K_s = 6.51$) and using the updated version of the 2MASS color transformations between 2MASS and CIT systems (Carpenter 2001), its estimated L' magnitude is 6.49. Both the ADI and LOCI reduction procedures attenuate some companion flux in the process of attenuating speckles. To further calibrate our photometry, we introduce and measure the flux for fake point sources at random angles at a range of separations ($0.5''$ – $2.5''$) in each registered frame, rerun our ADI and LOCI pipelines, compute the attenuated flux in the final ADI/LOCI-processed images, and correct for this attenuation ($\sim 30\%$ at GJ 758B’s position for the LOCI reduction, $\sim 10\%$ for ADI). GJ 758B has $L' = 15.97 \pm 0.19$, where our photometric errors accounts for 1) the intrinsic photometric uncertainty for GJ 758B, 2) the intrinsic photometric uncertainty for our calibration star, and 3) the differences in photometry between the ADI and LOCI-reduced images⁵. Using the T09 H band photometry, we then find $H-L' = 3.29 \pm 0.25$ for GJ 758B.

The $H-L'$ color provides a first-order estimate for GJ 758B’s temperature and spectral type (Table 1). GJ 758B is far redder than than expected if it were a L–T8 dwarf⁶. However, GJ 758B is comparable in color to Wolf 940B ($H-L' = 3.38$), a 3.5–6 Gyr-old, 570 K T8.5 dwarf companion to a higher-mass brown dwarf (Burningham et al. 2008). To derive GJ 758B’s effective temperature, we compare its colors to the colors predicted by the COND evolutionary models for its age range (Baraffe et al. 2003). Based on isochronal fitting and age-activity correlations (e.g. Takeda et al. 2007; Mamajek and Hillenbrand 2008), GJ 758 has an age between 0.7 Gyr (~ 1 Gyr) and 8.7 Gyr (see discussion in T09). The 0.7 Gyr lower limit is based on isochrone fitting from the Y^2 tracks (Takeda et al. 2007), which may be highly uncertain given that GJ 758 is on/near the main sequence and given systematic disagreements between different sets of isochrones. For simplicity, we assume an age range of 1 Gyr to 10 Gyr to cover the low end of the age range and the main sequence lifetime of a Sun-

⁵If if our second, candidate point source is indeed the object T09 identify as “GJ 758C”, its magnitude would be $L' = 16.01 \pm 0.38$; the 3σ limit at its location reported in T09 is ~ 16.03 . Regardless of whether our candidate detection of “GJ 758C” is real or is a speckle, the $H-L'$ color for the purported “GJ 758C” object must be bluer than ≈ 2.5 .

⁶See the sample compiled by S. Leggett: [HREF]<http://staff.gemini.edu/~sleggett/LTdata.html>

like star (Sackmann et al. 1993). For this age range, GJ 758B has an allowed temperature range of $\log(T_e) \sim 2.675\text{--}2.85$ or $T_e = 560^{+150}_{-90}$ K, where the extrema are determined from the $\pm 1\sigma$ values for the H-L' color (3.04 and 3.54) and a slight age dependent calibration between temperature and color.

The implied luminosity of GJ 758B as probed by the companion's absolute H band magnitude and H-L' color is broadly consistent with COND model predictions of GJ 758B's age range. For GJ 758B's H-L' color, the COND models at 5 and 10 Gyr predict an absolute H band magnitude of ≈ 18.4 and 18.2, respectively. At 1 Gyr, the COND models predict $M_H \approx 18.6$, though given the uncertainty in the H-L' color the predicted near-IR absolute magnitudes are still consistent with observations. Given our range in effective temperatures and comparing L/L_\odot and T_e from 1–10 Gyr for the COND models, the bolometric luminosity of GJ 758B is $\log(L/L_\odot) \approx -6.1^{+0.3}_{-0.2}$.

Figure 2 plots the predicted temperature evolution of 10.5–42 M_J companions compared to the temperatures of GJ 758B and other cool, substellar-mass objects above and below the deuterium-burning limit. GJ 758B has an inferred mass ranging from 10–20 M_J (at 1 Gyr) to $\sim 25\text{--}40$ M_J (at 10 Gyr), consistent with estimated mass for Wolf 940B (24–45 M_J). Within the context of the temperature evolution of substellar objects predicted by the COND models, GJ 758B is likely higher mass than 1RXS J162041-210524B (Lafreniere et al. 2008, 2010) and 2M 1207B (Chauvin et al. 2004). GJ 758B is consistent with being an older, cooler analogue to mid-L brown dwarfs in the Pleiades (e.g. BRB29) studied by Bihain et al. (2010, and references therein) and the recently discovered brown dwarf companion to PZ Tel, a 12 Myr-old 1.3 M_\odot star (Biller et al. 2010).

For most of the GJ 758B age range, the COND models yield estimated masses above the deuterium burning limit nominally separating planets from brown dwarfs. The more reliable age indicators, age-activity relations (e.g. Mamajek and Hillenbrand 2008; Barnes et al. 2007), suggest that GJ 758 is at least as old as the Sun, and perhaps as old as ~ 8.7 Gyr (T09). Thus, the mass of GJ 758B is most plausibly comparable to that of low-mass brown dwarfs, not high-mass planets.

We investigate the range of plausible orbital parameters with a Monte Carlo simulation following the method of T09. With three astrometric points spanning one year (Figure 3, left panel), the orbital properties of GJ 758B are better constrained: only 1.2% of the trial orbital solutions "fit" the data compared to $\sim 6\%$ based on only the 2009 data (T09). The best-estimated eccentricity is high ($e_{M.W.} \sim 0.73^{+0.12}_{-0.21}$), and the best-estimated inclination indicates that the orbit is viewed neither pole on nor edge on ($i_{M.W.} \sim 50^{+14}_{-22}^\circ$). The best-estimated semimajor axis is ~ 44 AU $^{+32}_{-14}$, or $\approx 60\%$ larger than its projected separation of ~ 28 AU.

4. Discussion

Our study recovers the detection of GJ 758B reported by T09 and demonstrates that it has a red H-L’ color consistent with being an ultra-cool ($T \approx 560$ K) low-luminosity companion to a solar-type star. This estimate is consistent with the low end of the temperature range (550–640 K) quoted by T09 based on assuming that the COND models accurately reproduce the fluxes of substellar mass objects in each near-IR bandpass, although the allowed temperature range is about the same as that quoted by T09, given our photometric errors. We also identify a second point source at a separation comparable to the putative “GJ 758C” companion reported by T09, though its detection has a low significance and it is likely a residual speckle. However, if this is the same object as that previously reported, it is not in a bound orbit around GJ 758.

Based on the COND evolutionary models, GJ 758B has a mass between $\sim 10 M_J$ and $40 M_J$. However, for most of GJ 758’s age range, especially for ages derived from more reliable methods, its inferred mass is greater than the deuterium burning limit. Thus, based on our analysis, it is then much more likely that GJ 758B is a low-mass brown dwarf companion than a planet if “planet” is defined by an object’s mass relative to the deuterium burning limit.

A separate, perhaps more physically motivated criterion for defining an object to be a “planet” is its formation history: whether or not it formed in a protoplanetary disk around a young star. Sophisticated numerical models for planet formation (Kenyon and Bromley 2009) necessary for testing formation theories have yet to be directly applied to systems with directly-imaged planets. However, analytical arguments show that forming GJ 758B by core accretion is possible only if gas accretion is exceptionally efficient. Using Equation 14 from Rafikov (2010), the minimum surface density of solids required to trigger core instability within the lifetime of the disk is $\approx 6 \times 10^{-2} \text{ g cm}^{-2}$ for a (long) protoplanetary disk lifetime of 5 Myr (Currie et al. 2009). This surface density is comparable to that for Rafikov’s Minimum Mass Solar Nebula profile at our best fit semimajor axis of 44 AU. Once a core has formed, the isolation mass to which a non-migrating gas giant could grow is $> 10\text{--}20 M_J$ in disks containing that quantity of gas. However, accreting $> 10\text{--}20 M_J$ of gas in a disk that cannot be more than $\sim 100 M_J$ in mass total (else the disk would be gravitationally unstable) requires the planet to accrete very efficiently. Companion formation by gravitational instability of the disk, in contrast, can only occur while the disk is still accumulating gas from the protostellar core, and preferentially forms companions with masses more similar to field brown dwarfs than jovian-mass planets (e.g. Kratter et al. 2010; Rafikov 2005).

Formation may also be possible earlier, during the fragmentation of the molecular cloud core that formed GJ 758: GJ 758B would then comprise the low-mass end of the binary

mass function. Core fragmentation can probably produce objects much less massive than GJ 758B (e.g. 5–10 M_J Todorov et al. 2010), so we consider this scenario to be a plausible one for forming GJ 758B in addition to fragmentation during the protostar phase. Future multiwavelength studies of GJ 758B will better constrain its temperature and atmospheric properties. Combined with improved age estimates derived from stellar rotation and activity, these data will better place GJ 758B within the context of directly imaged low-mass brown dwarfs useful for investigating the mass function of objects approaching the deuterium burning limit.

We thank the anonymous referee and Adam Kraus for suggestions that strengthened this paper and Adam Burgasser, Marc Kuchner, Scott Kenyon, and Jonathan Irwin for other useful discussions. T.C. is supported by a NASA Postdoctoral Fellowship, D. F. is supported by a Michelson Fellowship, and R. M.-C. is supported by an Institute for Theory and Computation Fellowship.

REFERENCES

- Baraffe, I., et al., 2003, *A&A*, 402, 701
- Barnes, S. A., 2007, *ApJ*, 669, 1167
- Bihain, G., et al., 2010, arXiv:1005.3249
- Biller, B., et al., 2010, *ApJ Letters* in press, arXiv:1007.4808
- Burgasser, A., 2004, *ApJS*, 155, 191
- Burningham, B., et al., 2009, *MNRAS*, 395, 1237
- Burningham, B., et al., 2010, *MNRAS*, 404, 1952
- Burrows, A., et al., 1997, *ApJ*, 491, 856
- Carpenter, J., 2001, *AJ*, 121, 2851
- Chauvin, G, et al., 2004, *A&A*, 425, 25L
- Chiang, E., Kite, E., et al., 2009, *ApJ*, 693, 734
- Currie, T., Hernandez, J., Irwin, J., et al., 2010, *ApJS*, 186, 191
- Currie, T., Lada, C. J, et al., 2009, *ApJ*, 698, 1

- Currie, T., Itoh, Y., Fukagawa, M., et al., 2010, in prep.
- Fabrycky, D., Murray-Clay, R., 2010, 710, 1408
- Hinz, P., et al., 2006, ApJ, 653, 1486
- Hinz, P., et al., 2010, ApJ, 716, 417
- Itoh, Y., et al., 2005, ApJ, 620, 984
- Kalas, P., et al., 2008, Science, 322, 1345
- Kenyon, S. J., Bromley, B., 2009, ApJ, 690, 140L
- Kratter, K., Murray-Clay, R., Youdin, A., 2010, ApJ, 710, 1375
- Kraus, A., et al., 2008, ApJ, 679, 762
- Lafreniere, D., et al., 2007, ApJ, 660, 770
- Lafreniere, D., et al., 2008, ApJ, 689, 153L
- Lafreniere, D., et al., 2010, arXiv:1006.3070
- Lagrange, A-M., et al., 2010, Science in press, arXiv:1006.3314
- Leggett, S., et al., 2010, 710, 1627
- Lodato, G., et al., 2005, MNRAS, 364, L91
- Luhman, K., et al., 2006, ApJ, 649, 894
- Mamajek, E., Hillenbrand, L. A., 2008, ApJ, 687, 1264
- Marois, C., et al., 2006, ApJ, 641, 556
- Marois, C., et al., 2008, ApJ, 673, 647
- Marois, C., et al., 2008, Science, 332, 1348
- Metchev, S., Hillenbrand, L., 2006, ApJ, 651, 1166
- Rafikov, R., 2005, ApJ, 621, 69L
- Rafikov, R., 2010, arXiv:1004.5139
- Sackman, I. J., et al., 1993, ApJ, 418, 457

Sivanandam, S., et al., 2006, SPIE, 6269, 27

Takeda, G., et al., 2007, ApJS, 168, 297

Thalmann, C., et al., 2009, ApJ, 707, 123L

Todorov, A., Luhman, K., et al., 2010, ApJ, 710, 84L

Tokunaga, A. T., 2000, in Allen’s Astrophysical Quantities, 4th edition, ed. A.N. Cox, Springer-Verlag (New York), p. 143

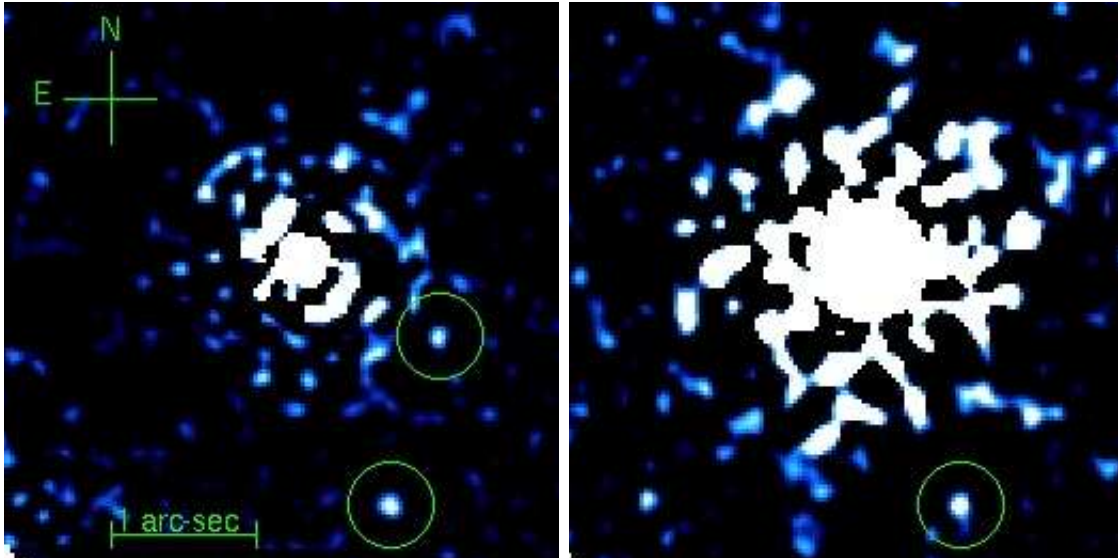


Fig. 1.— LOCI-reduced images from our May dataset (left) and June dataset (right) shown at high contrast to display residual speckle noise. GJ 758B (lower circle) is recovered in both data. A candidate point source with a separation comparable to that reported for “GJ 758C” (top circle, left panel) is also detected in the more sensitive May data, though this may instead be a residual speckle. Because of shorter integration times and far poorer field rotation, residual speckle noise is far more severe for the June data, and we do not recover the second, candidate point source.

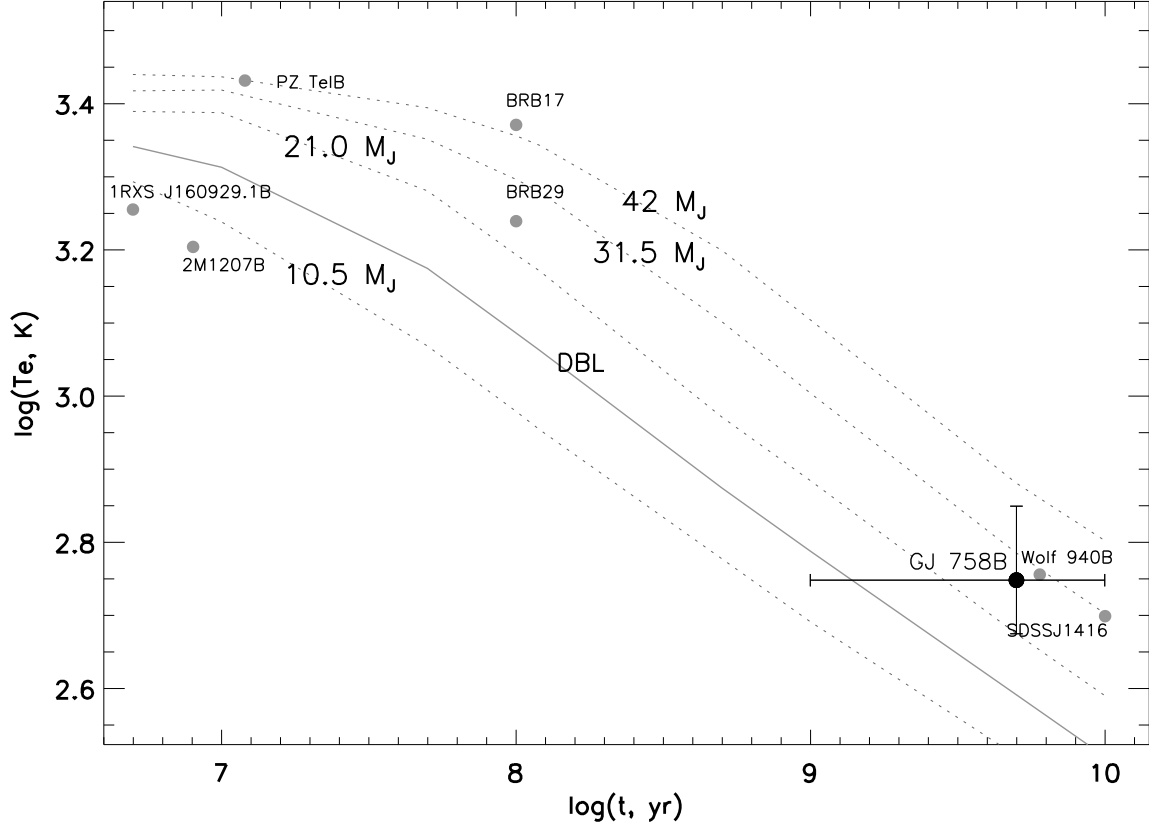


Fig. 2.— Effective temperature vs. age for low-mass brown dwarfs/planetary-mass objects orbiting solar and subsolar-mass stars. Along with GJ 758B, these include PZ Tel (Biller et al. 2010), 1RXS J160929.1B (Lafreniere et al. 2008, 2010), 2M 1207B (Chauvin et al. 2004), two L dwarfs in the Pleiades (Bihain et al. 2010), Wolf 940B (Burningham et al. 2008), and SDSS J1416+13AB (Burningham et al. 2009). We overplot the temperature evolution for 10.5–42 M_J objects from the COND evolutionary models (Baraffe et al. 2003).

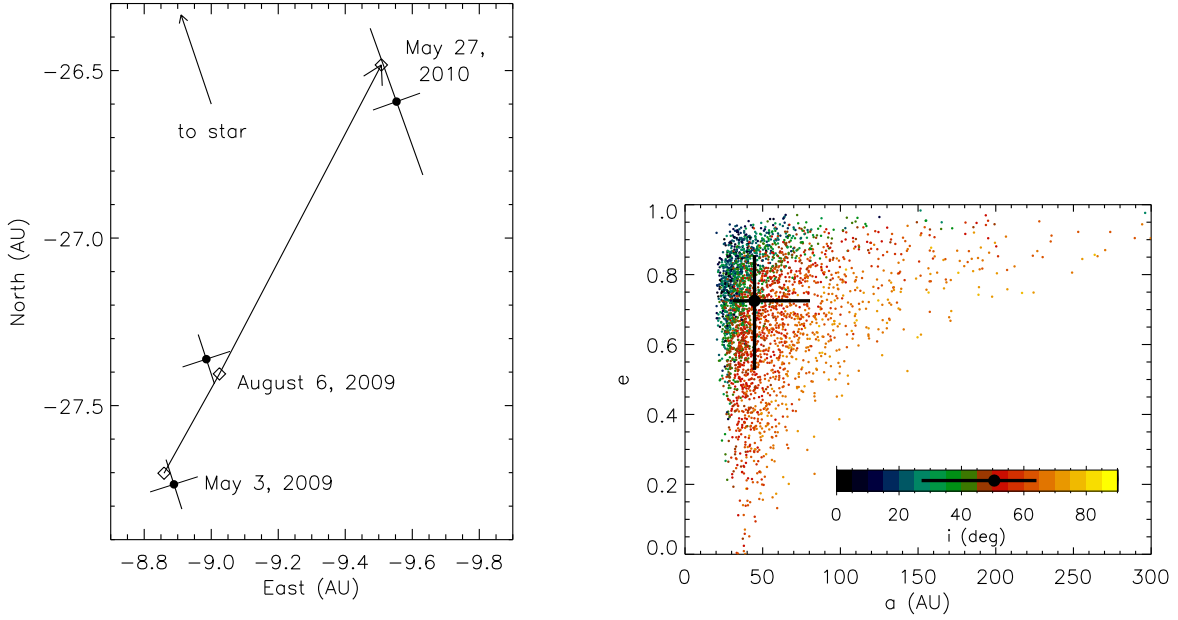


Fig. 3.— (left) Projected separation for GJ 758B between May 2009 and May 2010, combining our data (upper right) with that from T09. The arrows show the motion of GJ 758B from May 2009 (lower left) to May/June 2010 (upper right); the diamonds are the best-fit positions based on a rectilinear model. (right) Range of orbital solutions for GJ 758B following the method of T09.

Table 1. Observed and Derived Properties for GJ 758B

Properties	GJ 758B
Photometry	
App. L'	15.97 ± 0.19 mag
Abs. L'	14.84 ± 0.21 mag
H-L'	3.29 ± 0.25 mag
Derived Physical Properties	
Approx. Spectral Type	T8.5–T9
Te (inferred)	$\approx 560 +150, -90$ K
$\log(L/L_{\odot})$ (inferred)	$-6.1 +0.3, -0.2$
Inferred Mass (M_J) (1 Gyr)	10–20
(5 Gyr)	21.0–31.5
(10 Gyr)	25–40
Astrometry	
<i>May 3, 2009 (T09)</i>	
Separation (")	1.879 ± 0.005
Position Angle($^{\circ}$)	197.17 ± 0.15
<i>August 6, 2009 (T09)</i>	
Separation (")	1.858 ± 0.005
Position Angle($^{\circ}$)	198.18 ± 0.15
<i>May 27, 2010 (this work)</i>	
Separation (")	1.823 ± 0.015
Position Angle($^{\circ}$)	199.76 ± 0.15
Projected Separation (AU)	28.36
$\delta(\text{Sep., "})$	0.035
$\delta(\text{PA, }^{\circ})$	1.58
v_R	-0.9 ± 0.2 AU/yr
v_{PA}	0.94 ± 0.1 AU/yr
Derived Orbital Properties	
Semimajor Axis (AU)	44.12 (30.28, 76.66)
Eccentricity, Inclination	0.73 (0.52, 0.85), 49.64° (27.87° , 63.34°)

Note. — The changes in separation ($\delta\text{Sep.}$) and position angle (δPA) are given between our May 27, 2010 data and the August 6, 2009 data presented by T09. The semimajor axis, eccentricity, and inclination listed refers to the median-weighted value and the two values defining the inner 68% of weighted values. The instantaneous radial and angular velocities (v_R , v_{PA}) were determined at an epoch of 31 Dec 2009 (the error-weighted mean of our May datum and T09’s data) and an assumed distance of 15.5 pc.